Imaging Nitrogen in Individual Carbon Nanotubes

Jigang Zhou,*,[†] Jian Wang,*,[†] Hao Liu,[‡] Mohammad N. Banis,[‡] Xueliang Sun,[‡] and Tsun-Kong Sham*,[§]

[†]Canadian Light Source Inc., Saskatoon, Canada, [‡]Department of Mechanic and Materials Engineering, and [§]Department of Chemistry, The University of Western Ontario, London, Canada

ABSTRACT Semiquantitative chemical imaging of the spatial distribution of nitrogen in a carbon matrix, adsorbed/intercalated N_2, and highly concentrated N_2 in nitrogen-doped carbon nanotubes (N-CNTs) with a spatial resolution of 30 nm has been obtained by scanning transmission X-ray microscopy (STXM). The local electronic structures of individual N-CNTs at C and N K-edges have been extracted from STXM image stacks (sensitive to bulk) and compared with that of N-CNT using X-ray absorption near-edge structure spectroscopy in total electron yield mode (sensitive to surface). The polarization-dependent STXM measurement has revealed the preferred orientation of N_2, parallel to the N-CNT long axis.

SECTION Nanoparticles and Nanostructures

Nitrogen-doped carbon nanotubes (N-CNTs) have shown great promise in gas storage, energy conversion and storage, and electronics applications.[1−6] Moreover, first-principle simulations[7,8] have suggested that polymeric nitrogen (single-bonded nitrogen)[9] can be stabilized in carbon nanotubes, forming nanoscale energetic materials. It has been assumed that doping N in CNTs can produce such nanoenergetic materials. Nitrogen in N-CNTs exhibits a very broad range of structures such as graphitic-like, pyrridine-like, pyrrolic, cross-linked sp^3 structure, and gaseous N_2.[10−13] Different nitrogen sites play different roles in tailoring the structure of a N-CNT and hence its performance. Understanding and controlling the chemistry and electronic structure in N-CNTs is of foremost importance in achieving its promise in broad practical applications. To this end, being able to image the local chemistry and electronic structure variations within a single carbon nanotube is critical, but such information was apparently absent until now.[2−4,6] Considerable efforts have been made to identify the nitrogen chemistry in N-CNTs by electron energy loss spectroscopy (EELS),[1] X-ray photoelectron spectroscopy (XPS), and X-ray absorption near-edge structure (XANES) spectroscopy.[10,12−14] Radiation damage[1] and energy resolution limit the application of EELS, although it has high spatial resolution. In contrast, XANES spectroscopy is element-specific with high energy resolution and is sensitive to the local chemistry of the absorbing atom. It is also less susceptible to radiation damage. Although the electronic structures of N-CNTs have been investigated by XANES[10,12−14] studies, they only provide averaged information for a large sampling area.[2] Due to the difference in helicity, defects, and diameter, a bundle of N-CNTs inevitably has a much broader variation in electronic structure. Such variations can only be addressed by the spectromicroscopic study of an individual N-CNT. With the advent of the brilliant and polarization-controlled third-generation synchrotron sources, the state-of-the-art spectromicroscopic

technique, scanning transmission X-ray microscopy (STXM), provides an excellent combination of high spatial (30 nm) and energy resolution (resolving power up to 10000) as well as variable polarizations (linear to circular and elliptical) for chemical speciation. STXM has been successfully applied to the studies of the electronic structure and surface defects of individual CNTs[15−17] and a single catalyst under relevant operation conditions[18,19] and the chemical imaging of RuO_2 supported on carbon nanotubes.[20] This work reports an application of STXM to obtain the chemical imaging and the electronic structure of individual N-CNTs in considerably greater details than ever before. Specifically, the XANES of the N K-edge was used to image various N sites, the substituted N, adsorbed/intercalated N_2, and gaseous N_2 trapped in the cavity of a single N-CNT. Furthermore, the nitrogen and carbon chemistry on different locations of the N-CNT was studied by XANES at the N and C K-edges. High-resolution spectroscopy clearly shows the fine signatures of the vibronic N 1s $\rightarrow \pi^*$ transitions in molecular nitrogen encapsulated inside of the tube. Finally, the parallel orientation of N_2 in the N-CNT was revealed by polarized STXM.

N K-edge STXM image stacks of individual N-CNTs were fitted with two reference spectra, the N K-edge XANES of the N-CNTs (representing the substituted N, displayed in Figure 1d) and molecular N_2. Note that we observe N_2 molecules trapped inside of the N-CNT, and they are henceforth denoted condensed N_2, although part of them are most likely pressurized N_2 (see below). The chemical maps thus obtained are shown in Figure 1a (condensed N_2) and b (substituted N in a carbon matrix). It is obvious from the mapping in Figure 1a that the N_2 thickness varies among N-CNTs and even along individual
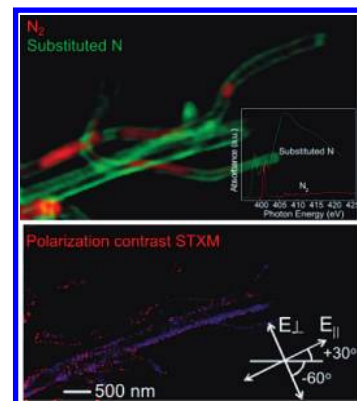
1709
DOI: 10.1021/jz100376v | *J. Phys. Chem. Lett.* **2010**, *1*, 1709–1713
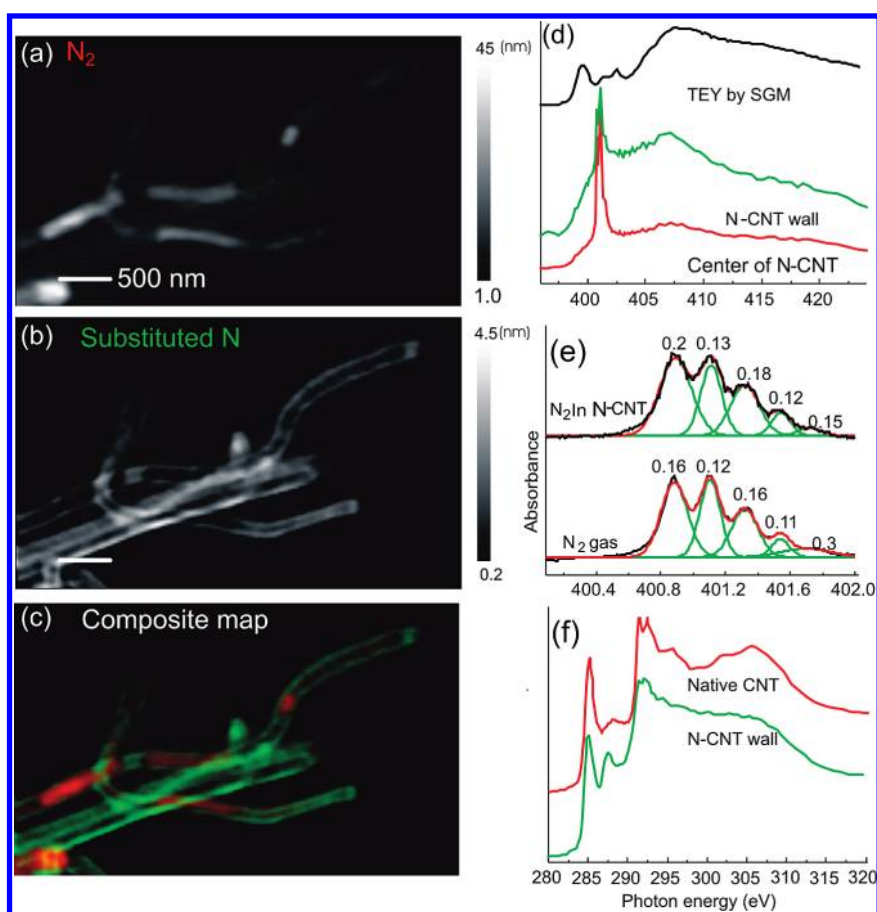
Figure 1. STXM chemical maps of N-CNTs: (a) quantitative chemical map of N_2, and (b) substituted N derived from the N 1s image stack; the vertical gray scale represents the thickness in nm in (a) and (b); (c) the colored composite map for relevant components (red: N_2; green: substituted N). The component maps are rescaled individually in each color channel. (d) Transmission XANES of the wall and the center regions of a N-CNT (N_2-rich regions) along with N K-edge XANES of N-CNTs recorded in TEY mode; (e) high-resolution N K-edge XANES spectra of N_2 gas and N_2 in N-CNTs obtained by STXM point spectrum (single pixel) scans. The peak width is labeled along with each peak. The fit for the first four peaks are at least semiquantitative. (f) C K-edge XANES of the wall of a N-CNT and a native CNT.

N-CNTs. A thin layer of N_2 (less than 5 nm of condensed N_2) is widely and evenly distributed over the N-CNTs, which is considered to be the adsorbed/intercalated N_2 located within and on the inner surface of the tube wall. More highly concentrated N_2 (about 20−45 nm of condensed N_2) is distributed in some isolated regions, suggesting that molecular N_2 is trapped inside of the tube compartments. Such high-concentration N_2 (equivalent to 15−40 nm of condensed N_2 after removing the contribution from adsorbed/intercalated N_2 in the wall) sealed in CNTs with an inner diameter of about 100 nm indicates a very high pressure (estimated to be ∼50 atm by scaling to the absorbance of gaseous N_2 with a known pressure). The molecular nature of the high-concentration N_2 is revealed by the high energy resolution vibronic structures of the N 1s → π^* transitions, as shown in Figure 1e. The distribution of highly concentrated N_2 among N-CNTs highlights their structural variation. From Figure 1b, a quantitative map of substituted N in N-CNTs, a number of interesting observations are apparent. First, substituted N occurs more evenly along the N-CNT. Second, the compartment membranes in the bamboo-like structure (which has been observed by transmission electron microscopy in Supporting Information Figure S4) are

well-resolved just like that of the tubular structure, which means that substituted N also presents in the compartment membranes. Finally, the doping of nitrogen inside of the carbon nanotube is about 1−2 nm across the tube wall. The color composite map of N_2 and substituted N in the individual N-CNTs is displayed in Figure 1c.

In addition to chemical mapping, STXM probes the electronic structure locally (e.g., in a single pixel), that is, nanospectroscopy. Figure 1d compares the N K-edge transmission XANES of the wall and the center of an individual N-CNT (N_2 rich regions) along with XANES obtained by TEY (average of many N-CNTs). The XANES at the wall and the center of the N-CNT extracted from the STXM image stack features the N_2 1s → π^* resonance around 401 eV and the substituted N (corresponding to the pre-edge features before the N_2 vibration 1s → π^* structure). Due to the N_2 contribution, the substituted N can only be uniquely observed as a pre-edge which is more obvious in the tube wall; therefore, the detailed chemistry of substituted N has been studied by TEY XANES. The sharp resonance peaks below a broad peak at ∼407 eV (transition into the σ^* states and sensitive to the bond length between N and C[11−13,21]) arise from transitions from the K shell (N 1s) to unoccupied π^*

orbitals containing N 2p character. This is undoubtedly direct evidence of successful nitrogen doping into the carbon matrix, forming unsaturated C−N bonds in N-CNTs. Three π^* peaks at 399, 401, and 402.6 eV are attributed to the pyridine-like (though this peak could also be the cyanide-like structure, but this does not agree with our XPS results[22]) and graphite-like N or N_2 and oxidized pyridine-like bonding in nitrogenated carbon materials.[11−13,21] The high-resolution vibrational structure of a highly concentrated N_2 region (Figure 1e) presents the high energy resolution feature in STXM which was not observed in EELS. Similar vibrational fine structure in N_2 molecular clusters has been reported.[23] The broadening of the first four vibrational features in N_2 sealed in a N-CNT relative to that of gaseous N_2 supports the high N_2 pressure in N-CNTs. The effect of N substitution on N-CNTs was also studied by C K-edge XANES extracted from C K-edge STXM stacks. The XANES at the N-CNT wall was compared to the C K-edge XANES from a native CNT, as shown in Figure 1f. The π^* transition at 285.1 eV and σ^* at 291.5 and 292.5 eV are characteristic of the graphite structure. In between those transitions, a relatively broad peak at 288.3 eV appears in the XANES of the CNT, which indicates the existence of a carboxylic group.[21] In contrast, a rather sharp transition peak at 287.5 eV is displayed in XANES from the wall of the N-CNT. This spectroscopic signature should be due to the pyridine-like N substitution in a carbon matrix. The π^* transition in the N-CNT also shifts slightly to lower energy. The shift is accompanied by a reduction in intensity. All of these observations indicate electron doping by the substituted N.

Furthermore, polarized STXM[17] was applied to study the orientation of nitrogen in N-CNTs. It was performed by applying the linear inclined polarization parallel (+30°) and perpendicular (−60°) to the selected N-CNT's long axis (see Figure 2 and Supporting Information Figure S3). Then, well-focused individual images were taken at selected energies for each polarization. The polarization dependence was evaluated based on the normalized intensity ratio of $I_\parallel/I_\perp$ for the π^* feature. The polarization maps of N-CNT and N_2 at the C and N π^*, respectively, were generated by subtracting images with the beam **E** vector (−60°) perpendicular to the tube by images with the beam **E** vector (+30°) parallel to the tube. (The detailed polarization experiment and analysis are described in the Supporting Information). Figure 2a and b display the distribution of polarized N_2 and N-CNTs, respectively. A color composite polarization map (Figure 2c) of N_2 (in red) and N-CNT (in blue) was made to guide the visualization of the polarization effect. It clearly shows a strong correlation of the polarized N_2 related to the N-CNT tube wall. Such a polarization effect suggests that polarized N_2 aligns along the tube's long axis as carbon in N-CNT does. The low polarization dependence of N_2 (0.86, Supporting Information Table S1) correlates with the low polarization dependence of the N-CNT at the carbon K-edge (0.79, Supporting Information Table S1) (a native CNT with a polarization dependence of 0.3;[17] the low polarization at the C K-edge in the N-CNT is due to its intrinsic low crystallinity[22]). This correlation hints that the molecular axis of the adsorbed and intercalated N_2 are oriented with respect to the wall of the N-CNT as a template.
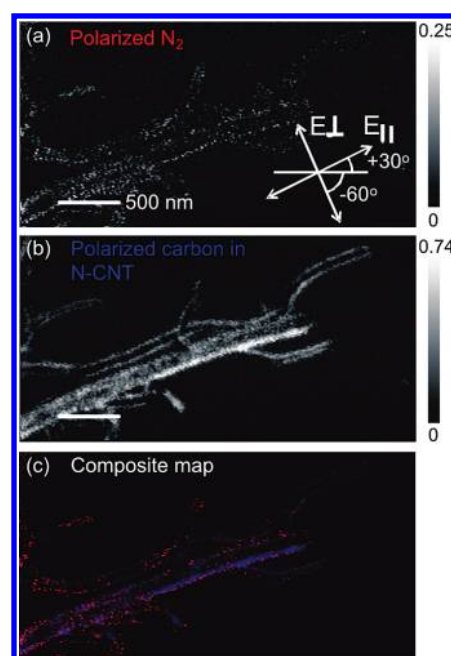
Figure 2. Polarization maps of N_2 and carbon in N-CNTs derived from the N and C π^* resonance by STXM. (a) The polarization map of N_2 obtained at the N π^* (401.1 eV) by subtracting images with the beam **E** vector (−60°) perpendicular to the tube by images with the beam **E** vector (+30°) parallel to the tube; (b) the polarization map of carbon in the N-CNT obtained at the C π^* (285.1 eV); the vertical gray scale represents the absorbance (i.e., optical density); (c) the colored composite map for components (red: polarized N_2; blue: polarized N-CNT). The component maps are rescaled individually in each color channel.

In summary, we have reported the chemical mapping of different N components of individual N-CNTs obtained by STXM with a spatial resolution of 30 nm. We have identified substitutional N, N_2 adsorbed and intercalated between graphene walls, and molecular N_2 trapped in bamboo-like compartments. XANES spectra at the N K-edge and C K-edge of individual N-CNTs have been used to reveal the electronic structure variation within individual N-CNTs and among N-CNTs. Furthermore, the polarized STXM confirms the presence of sporadic regions of polarized N_2 near the CNT walls, which might be relevant to a parallel orientation of adsorbed and intercalated N_2 to the tube's long axis.

METHODS

Nitrogen-doped carbon nanotube arrays (N-CNTs) were prepared by the floating catalyst chemical vapor deposition method. The details of preparation can be found elsewhere.[22] Briefly, 100 mg of ferrocene was used as the precursor to produce metallic iron and melamine as the nitrogen source in making N-CNTs on a Si wafer. The N-CNTs thus obtained have been characterized to contain 8 % nitrogen using XPS.[22] The morphology of the N-CNT was studied by transmission electron microscopy (TEM) imaging using a Philips CM10 TEM microscope operating at 80 KeV. To perform STXM, the N-CNT sample was scratched from the Si substrate and predispersed in methanol and then deposited on Si_3N_4 windows (thickness 75 nm, Norcada Inc.) using a micropipet. The STXM was

performed on the SM beamline at the Canadian Light Source (CLS), a 2.9 GeV third-generation synchrotron source. The beamline is equipped with an APPLE II type elliptically polarizing undulator (EPU), which provides circularly polarized light (up to 1000 eV) and linearly polarized light (130−2500 eV) with polarization adjustable from +90 to −90°. The STXM principle and the design of the microscope have been described elsewhere.[24] In short, the monochromatic X-ray beam is focused by a Fresnel zone plate to a 30 nm spot (this work) on the sample. The sample is raster-scanned with synchronized detection of transmitted X-rays to generate images. Chemical imaging and XANES spectra are obtained using image sequence (stack) scans[25] over a range of photon energies at a specific element edge. The X-ray photon energy scale was calibrated by a gas-phase XANES spectrum of N_2 in the N K-edge. STXM data were analyzed by aXis2000 (it is an application written in Interactive Data Language and available free for noncommercial applications at http://unicorn.mcmaster.ca/aXis2000.html). Chemical component maps were obtained by fitting the N K-edge image stacks with linear reference spectra of N_2 and substituted N in N-CNTs. High energy resolution point spectra with an energy step of 0.01 eV were acquired on the N-CNT specific regions, that is, high-concentration trapped N_2 regions as determined by chemical mapping through STXM stacks, with normalization to the I_0 spectrum obtained simultaneously at a blank region on the same Si_3N_4 window close to the N-CNT region. XANES of substituted N in N-CNTs was obtained by studying a N-CNT array at the SGM beamline of the CLS. The polarization dependence was obtained by applying the linear inclined polarization parallel and perpendicular to specifically selected N-CNTs. More details of the STXM experiment and data analysis are described in the Supporting Information.

SUPPORTING INFORMATION AVAILABLE
STXM experiment, data analysis, Figure S1, S2, S3, and S4, and Table S1. This material is available free of charge via the Internet at http://pubs.acs.org.

AUTHOR INFORMATION

Corresponding Author:
*To whom correspondence should be addressed. E-mail: jigang.zhou@lightsource.ca (J.Z.); jian.wang@lightsource.ca (J.W.); tsham@uwo.ca (T.-K.S.).

REFERENCES

(1) Terrones, M.; Kamalakaran, R.; Seeger, T.; Ruhle, M. Novel Nanoscale Gas Containers: Encapsulation of N_2 in CN_x Nanotubes. *Chem. Commun.* **2000**, 2335–2336.

(2) Ghosh, K.; Kumar, M.; Maruyama, T.; Ando, Y. Micro-Structural, Electron-Spectroscopic and Field-Emission Studies of Carbon Nitride Nanotubes Grown from Cage-Like and Linear Carbon Sources. *Carbon* **2009**, *47*, 1565–1575.

(3) Ghosh, K.; Kumar, M.; Maruyama, T.; Ando, Y. Tailoring the Field Emission Property of Nitrogen-Doped Carbon Nanotubes by Controlling the Graphitic/Pyridinic Substitution. *Carbon* **2010**, *48*, 191–200.

(4) Gong, K. P.; Du, F.; Xia, Z. H.; Durstock, M.; Dai, L. M. Nitrogen-Doped Carbon Nanotube Arrays with High Electrocatalytic Activity for Oxygen Reduction. *Science* **2009**, *323*, 760–764.

(5) Wiggins-Camacho, J. D.; Stevenson, K. J. Effect of Nitrogen Concentration on Capacitance, Density of States, Electronic Conductivity, and Morphology of N-Doped Carbon Nanotube Electrodes. *J. Phys. Chem. C* **2009**, *113*, 19082–19090.

(6) Zhong, Z.; Lee, G. I.; Bin Mo, C.; Hong, S. H.; Kang, J. K. Tailored Field-Emission Property of Patterned Carbon Nitride Nanotubes by a Selective Doping of Substitutional N(Sn) and Pyridine-Like N(Pn) Atoms. *Chem. Mater.* **2007**, *19*, 2918–2920.

(7) Abou-Rachid, H.; Hu, A. G.; Timoshevskii, V.; Song, Y. F.; Lussier, L. S. Nanoscale High Energetic Materials: A Polymeric Nitrogen Chain N_8 Confined inside a Carbon Nanotube. *Phys. Rev. Lett.* **2008**, *100*, 196401(1)–196401(3).

(8) Ji, W.; Timoshevskii, V.; Guo, H.; Abou-Rachid, H.; Lussier, L. S. Thermal Stability and Formation Barrier of a High-Energetic Material N_8 Polymer Nitrogen Encapsulated in(5,5) Carbon Nanotube. *Appl. Phys. Lett.* **2009**, *95*, 021904(1)–021904(3).

(9) Eremets, M. I.; Gavriliuk, A. G.; Trojan, I. A.; Dzivenko, D. A.; Boehler, R. Single-Bonded Cubic Form of Nitrogen. *Nat. Mater.* **2004**, *3*, 558–563.

(10) Czerw, R.; Terrones, M.; Charlier, J. C.; Blase, X.; Foley, B.; Kamalakaran, R.; Grobert, N.; Terrones, H.; Tekleab, D.; Ajayan, P. M..; et al. Identification of Electron Donor States in N-Doped Carbon Nanotubes. *Nano Lett.* **2001**, *1*, 457–460.

(11) Choi, H. C.; Bae, S. Y.; Jang, W. S.; Park, J.; Song, H. J.; Shin, H. J.; Jung, H.; Ahn, J. P. Release of N_2 from the Carbon Nanotubes Via High-Temperature Annealing. *J. Phys. Chem. B* **2005**, *109*, 1683–1688.

(12) Choi, H. C.; Park, J.; Kim, B. Distribution and Structure of N Atoms in Multiwalled Carbon Nanotubes Using Variable-Energy X-ray Photoelectron Spectroscopy. *J. Phys. Chem. B* **2005**, *109*, 4333–4340.

(13) Yang, J. H.; Lee, D. H.; Yum, M. H.; Shin, Y. S.; Kim, E. J.; Park, C. Y.; Kwon, M. H.; Yang, C. W.; Yoo, J. B.; Song, H. J..; et al. Encapsulation Mechanism of N_2 Molecules into the Central Hollow of Carbon Nitride Multiwalled Nanofibers. *Carbon* **2006**, *44*, 2219–2223.

(14) Choi, H. C.; Bae, S. Y.; Park, J.; Seo, K.; Kim, C.; Kim, B.; Song, H. J.; Shin, H. J. Experimental and Theoretical Studies on the Structure of N-Doped Carbon Nanotubes: Possibility of Intercalated Molecular N_2. *Appl. Phys. Lett.* **2004**, *85*, 5742–5744.

(15) Felten, A.; Bittencourt, C.; Pireaux, J. J.; Reichelt, M.; Mayer, J.; Hernandez-Cruz, D.; Hitchcock, A. P. Individual Multiwall Carbon Nanotubes Spectroscopy by Scanning Transmission X-Ray Microscopy. *Nano Lett.* **2007**, *7*, 2435–2440.

(16) Felten, A.; Hody, H.; Bittencourt, C.; Pireaux, J. J.; Cruz, D. H.; Hitchcock, A. P. Scanning Transmission X-ray Microscopy of Isolated Multiwall Carbon Nanotubes. *Appl. Phys. Lett.* **2006**, *89*, 093123(1)–093123(3).

(17) Najafi, E.; Cruz, D. H.; Obst, M.; Hitchcock, A. P.; Douhard, B.; Pireaux, J. J.; Felten, A. Polarization Dependence of the C 1s X-ray Absorption Spectra of Individual Multi-Walled Carbon Nanotubes. *Small* **2008**, *4*, 2279–2285.

(18) de Smit, E.; Swart, I.; Creemer, J. F.; Hoveling, G. H.; Gilles, M. K.; Tyliszczak, T.; Kooyman, P. J.; Zandbergen, H. W.;

Morin, C.; Weckhuysen, B. M..; et al. Nanoscale Chemical Imaging of a Working Catalyst by Scanning Transmission X-ray Microscopy. *Nature* **2008,** *456,* 222–225.

(19)   de Smit, E.; Swart, I.; Creemer, J. F.; Karunakaran, C.; Bertwistle, D.; Zandbergen, H. W.; de Groot, F. M. F.; Weckhuysen, B. M. Nanoscale Chemical Imaging of the Reduction Behavior of a Single Catalyst Particle. *Angew. Chem., Int. Ed.* **2009,** *48,* 3632–3636.

(20)   Zhou, J. G.; Wang, J.; Fang, H. T.; Wu, C. X.; Cutler, J. N.; Sham, T. K. Nanoscale Chemical Imaging and Spectroscopy of Individual RuO_2 Coated Carbon Nanotubes. *Chem. Commun.* **2010,** *46,* 2778–2780.

(21)   Zhou, J. G.; Zhou, X. T.; Li, R. Y.; Sun, X. L.; Ding, Z. F.; Cutler, J.; Sham, T. K. Electronic Structure and Luminescence Center of Blue Luminescent Carbon Nanocrystals. *Chem. Phys. Lett.* **2009,** *474,* 320–324.

(22)   Liu, H.; Zhang, Y.; Li, R. Y.; Sun, X. L.; Desilets, S.; Abou-Rachid, H.; Jaidann, M.; Lussier, L. S. Structural and Morphological Control of Aligned Nitrogen-Doped Carbon Nanotubes. *Carbon* **2010,** *48,* 1498–1507.

(23)   Flesch, R.; Pavlychev, A. A.; Neville, J. J.; Blumberg, J.; Kuhlmann, M.; Tappe, W.; Senf, F.; Schwarzkopf, O.; Hitchcock, A. P.; Ruhl, E. Dynamic Stabilization in $1\,\sigma_u \rightarrow 1\,\pi_g$ Excited Nitrogen Clusters. *Phys. Rev. Lett.* **2001,** *86,* 3767–3770.

(24)   Kilcoyne, A. L. D.; Tyliszczak, T.; Steele, W. F.; Fakra, S.; Hitchcock, P.; Franck, K.; Anderson, E.; Harteneck, B.; Rightor, E. G.; Mitchell, G. E. Interferometer-Controlled Scanning Transmission X-ray Microscopes at the Advanced Light Source. *J. Synchrotron Radiat.* **2003,** *10,* 125–136.

(25)   Jacobsen, C.; Wirick, S.; Flynn, G.; Zimba, C. Soft X-Ray Spectroscopy from Image Sequences with Sub-100 nm Spatial Resolution. *J. Microsc. (Oxford, U.K.)* **2000,** *197,* 173–184.